

New version of Log-Logistic distribution: properties and applications to survival time and demographic data

Arjun Kumar Gaire¹

ABSTRACT

This paper proposes a Deflation-Inflation Log-Logistic (DILLog) distribution as a sub-model of the Deflation-Inflation Distributed (DID) family, introduced by Alodat and Al-Rawwash (2021). The proposed model offers greater flexibility than the original model in fitting data from real-world problems, especially for survival times and demographic data. The DILLog model is characterized by unimodal right-tailed density and hazard rate functions, and its key statistical properties, including the cumulative distribution function and a closed-form quantile function, are derived. To test the performance of the distribution, a simulation study has been used as well as an application to two real data sets: the age at menarche of Nepalese girls and the survival times of patients suffering from melanoma disease. To illustrate the usefulness and application of the proposed distribution, its parameters were estimated by using the maximum likelihood estimation method. The analysis and plots of the fitted results attest to the the DILLog model being flexible enough to fit the right-skewed real data. The actual application of demographic and survival datasets demonstrates that the DILLog distribution outperforms comparative models.

Key words: deflation-inflation, log-logistic, melanoma, menarche, survival

1. Introduction

In the recent literature on univariate probability distributions, various researchers, statisticians, and mathematicians have introduced numerous new distributions. These include pioneering new families and modifying the existing distribution by adding extra parameters, such as shape, scale, location, or threshold, to the original distribution. They aimed to meet the increasing demand for a flexible distribution in various aspects of everyday life. Such modified distributions have been applied to model a wide range of fields, including economics, physics, bio-statistics, engineering, and many others. Recently, such new distributions have been utilized in actuarial data analysis (Mohammad and Cooray, 2024), demography (Gaire and Aryal, 2015; Gaire et al., 2022; Gaire, 2023; Gaire et al., 2024a), and various other applications reported in the literature. In this study, a new Deflation-Inflation Log-Logistic (DILLog) distribution is introduced, based on the Deflation-Inflation (DI) distribution, the concept proposed by Alodat and Al-Rawwash (2021). Further, some statistical properties of the distribution have been formulated to illustrate its flexibility and applicability. Two real data sets of the age at menarche of Nepalese girls and the survival time of patients suffering from melanoma disease have been applied. The results of data fitting using

¹ Department of Science and Humanities, Khwopa Engineering College, Purbanchal University, Bhaktapur, Nepal. E-mail: arjun.gaire@gmail.com. ORCID: <https://orcid.org/0000-0002-1958-9797>.

the new model were compared to those of the LLog, Transmuted LLog (TrLLog), and Kumaraswamy LLog (KuLLog) distributions. Akaike's information criteria (AIC), Bayesian information criteria (BIC), Kolmogorov-Smirnov (KS) test, and Anderson-Darling (AD) test have been used to test the significance of fitting the data sets. The proposed model is found to be more flexible and a better fit to the data than the selected probability distributions.

The rest of the manuscript is organized as follows. Section 2 introduces a new DILLog distribution that has been formulated. In Section 3, some statistical properties and the rule for generating random numbers are derived. Section 4 includes the methods of parameter estimation. Section 5 presents the simulation study, and Section 6 contains the numerical application and model validation using two actual sets. Finally, section 7 concludes the manuscript.

2. Model formulation

In this study, a new univariate statistical distribution, named the DILLog distribution, is formulated by applying the DI-family of distributions (Alodat and Al-Rawwash, 2021). The cumulative density function (CDF) and probability density function (PDF) of the DI-family of distribution are expressed in Equations 1 and 2 as follows:

$$F(x) = \frac{\ln[1 + \lambda G(x)]}{\ln(1 + \lambda)} \quad (1)$$

$$f(x) = \frac{\lambda g(x)}{\ln(1 + \lambda)(1 + \lambda G(x))}, \quad \lambda > -1 \quad (2)$$

where the $g(x)$ and $G(x)$ are the PDF and CDF of the base distribution to be chosen. In the DI-family of distribution, the parameter λ is called the inflation-deflation parameter and controls how the new distribution deviates from the baseline distributions. When $\lambda = 0$, the DI distribution reduces to the baseline distribution, which means no inflation or deflation occurs. When $\lambda > 0$, the DI distribution exhibits inflation of the base PDF in the tail or central region. It increases the tail's heaviness, making large values more likely. Further, with the value of the parameter in the range $-1 < \lambda < 0$, the distribution exhibits deflation, reducing the PDF in the tails or central regions so that it produces lighter tails than the baseline distribution (Alodat and Al-Rawwash, 2021, P. 3). In this study, the LLog distribution is chosen as a base distribution. Because of the flexible nature of the LLog distribution, it has been used to modeling different real-world problems and also has been chosen as a base distribution in different generalized and modified versions such as Kumaraswamy LLog (De-Santana et al., 2012), Beta LLog (Lemonte, 2014) using the concept of Eugene et al. (2002) and Jones (2004), Transmuted LLog (Aryal, 2013), Marshall-Olkin extended LLog (Gui, 2013). Further, Zografos-Balakrishnan LLog (Hamedani, 2013), McDonald LLog (Tahir et al., 2014), Additive Weibull LLog (Hemeda, 2018), Transmuted generalized LLog (Adeyinka et al., 2019), Skew LLog (Gaire et al., 2019, Gaire and Gurung, 2024b),

and Rayleigh Generated LLog (Gaire and Gurung, 2024a). In the same line, in this study, the LLog distribution has been chosen as the base distribution to formulate a four-parameter DILLog distribution as a special case of the DI-family of distribution.

The PDF and the CDF of the three-parameter LLog distribution are given as:

$$g(x) = \frac{\alpha}{\beta} \frac{\left(\frac{x-\gamma}{\beta}\right)^{\alpha-1}}{\left(1 + \left(\frac{x-\gamma}{\beta}\right)^\alpha\right)^2} \tag{3}$$

$$G(x) = \frac{\left(\frac{x-\gamma}{\beta}\right)^\alpha}{1 + \left(\frac{x-\gamma}{\beta}\right)^\alpha} \tag{4}$$

where the first constant $\alpha > 0$ is the shape parameter, the second constant $\beta > 0$ is the scale parameter, and the third constant $x > \gamma$ is the location parameter. In many cases, we need a threshold parameter to guarantee that no failure occurs before a given time. Here, we chose the LLog distribution with the third parameter $\gamma > 0$, since many research studies report positive data exceeding a certain threshold. For example, the age of a girl at menarche is, of course, greater than zero.

After substituting the value of $g(x)$ and $G(x)$ of the LLog distribution in Equations 1 and 2, the CDF and PDF of the DILLog distribution are obtained and expressed in Equations 5 and 6 as follows. Both the CDF and PDF satisfy the required validity conditions, with the CDF meeting the boundary conditions and the PDF being non-negative and integrating to unity over the specified range $(0, \infty)$.

$$F(x) = \frac{1}{\ln(1 + \lambda)} \ln \left(\frac{1 + (1 + \lambda) \left(\frac{x-\gamma}{\beta}\right)^\alpha}{1 + \left(\frac{x-\gamma}{\beta}\right)^\alpha} \right) \tag{5}$$

$$f(x) = \frac{\alpha \lambda \left(\frac{x-\gamma}{\beta}\right)^{\alpha-1}}{\beta \ln(1 + \lambda) \left(1 + \left(\frac{x-\gamma}{\beta}\right)^\alpha\right) \left(1 + (1 + \lambda) \left(\frac{x-\gamma}{\beta}\right)^\alpha\right)}, \quad x > \lambda, \alpha, \beta > 0, \lambda > -1 \tag{6}$$

The PDF and CDF of the DILLog distribution for selected parameter values are plotted in Figures 1 and 2, respectively.

The reliability function $R(x)$, which is the probability of an item not failing before some time x , is defined by $R(x) = 1 - F(x)$. Thus, the reliability function of a DILLog probability distribution is given in Equation 7, and its visual representation is shown in Figure 3.

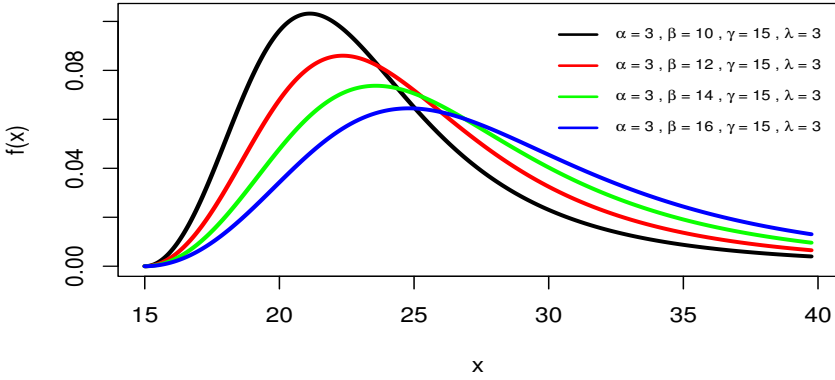


Figure 1. Plots of the PDF of DILLog distribution for different value parameters

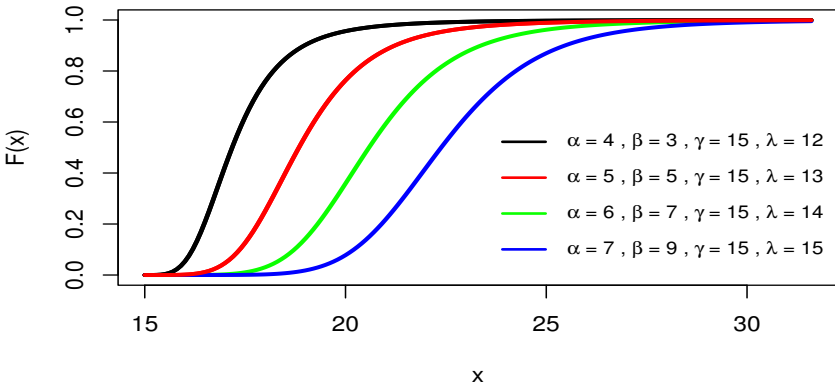


Figure 2. Graph of the CDF of DILLog for different values of parameters

$$R(x) = 1 - \frac{1}{\ln(1 + \lambda)} \ln \left(\frac{1 + (1 + \lambda) \left(\frac{x-\gamma}{\beta}\right)^\alpha}{1 + \left(\frac{x-\gamma}{\beta}\right)^\alpha} \right) \tag{7}$$

The conditional probability of failure assuming that it has survived up to the time x is given by the hazard rate function defined by $h(x) = \frac{f(x)}{1-F(x)}$. The hazard rate function of the DILLog distribution is given by Equation 8, and its graphical representation is shown in Figure 4. The hazard rate curve exhibits a rapidly increasing unimodal shape. Then it decreases steadily to attain the right-tailed curve, suggesting that this shape is suitable for modeling right-tailed data.

$$h(x) = \frac{\alpha\lambda}{\beta} \cdot \frac{\left(\frac{x-\gamma}{\beta}\right)^{\alpha-1} \left[\ln \left(\frac{1 + \left(\frac{x-\gamma}{\beta}\right)^\alpha}{\ln(1+\lambda) \left(1 + (1+\lambda) \left(\frac{x-\gamma}{\beta}\right)^\alpha\right)} \right) \right]^{-1}}{\left(1 + \left(\frac{x-\gamma}{\beta}\right)^\alpha\right) \left(1 + (1 + \lambda) \left(\frac{x-\gamma}{\beta}\right)^\alpha\right)} \tag{8}$$

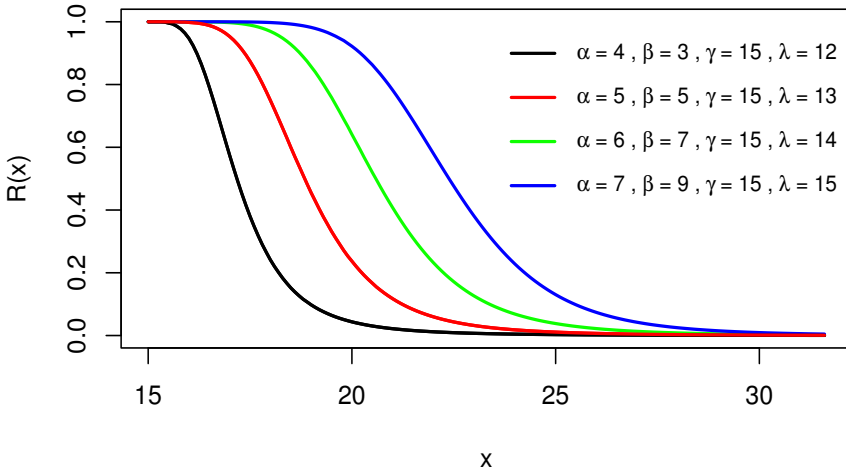


Figure 3. The plot of the reliability function of the DILLog probability distribution

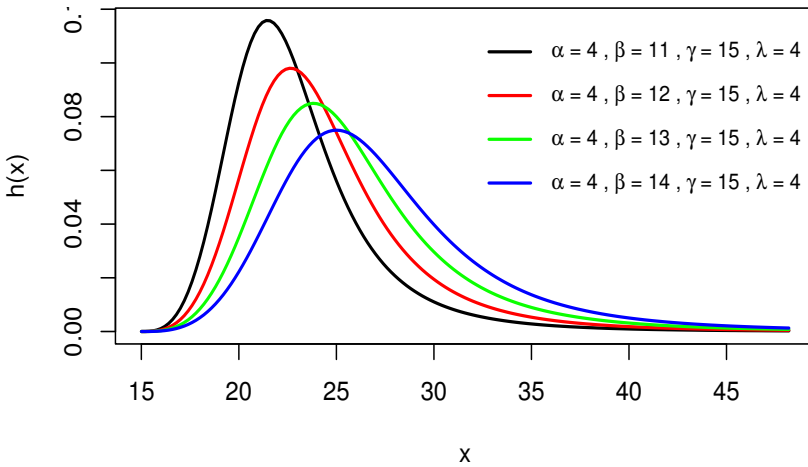


Figure 4. Plot of hazard rate function of DILLog distribution

The cumulative hazard rate function defined by $H(x) = -\ln[R(x)]$ of the DILLog distribution has been expressed in Equation 9 and is illustrated graphically in Figure 5. All of these functions support survival and reliability testing, actuarial data modeling, demographic data modeling, and numerous other fields.

$$H(x) = \text{Ln} \left[1 - \frac{1}{\ln(1 + \lambda)} \ln \left(\frac{1 + (1 + \lambda) \left(\frac{x - \gamma}{\beta} \right)^\alpha}{1 + \left(\frac{x - \gamma}{\beta} \right)^\alpha} \right) \right] \tag{9}$$

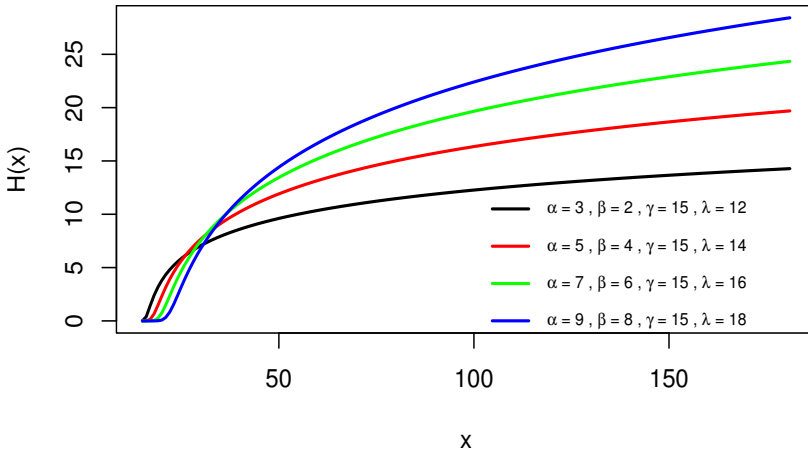


Figure 5. Graph of cumulative hazard rate function for different values of parameters

3. Statistical properties

In this section of this research, some structural properties of the DILLog distribution were presented.

3.1. Linear representation

For a more straightforward calculation of statistical features and further use of this model, the linear representations of the PDF and CDF of the DILLog distribution were presented. For this, the following series expansions were used.

The Taylor series expansion of the natural logarithm, given in Equation 10, where $m \in N$ is a positive integer.

$$\ln(1+x) = \sum_{m=1}^{\infty} \frac{(-1)^{m+1} x^m}{m}, \text{ for } |x| < 1 \tag{10}$$

Also, the geometric series expansion is expressed in Equation 11, where $j \in N_0$ is a non-negative integer.

$$(1+x)^{-1} = \sum_{j=0}^{\infty} (-1)^j x^j, \text{ for } |x| < 1 \tag{11}$$

Using these expansions Equation 12 represents the expanded form of the PDF and Equation 13 represents the expanded form CDF of DILLog distributions, where $m \in N$, and $i, j \in N_0$.

$$f(x) = \frac{\alpha \lambda}{\beta \ln(1+\lambda)} \sum_{i=0}^{\infty} \sum_{j=0}^{\infty} (-1)^{i+j} (1+\lambda)^j \left(\frac{x-\gamma}{\beta} \right)^{\alpha(i+j+1)-1} \tag{12}$$

$$F(x) = \frac{1}{\ln(1 + \lambda)} \sum_{m=1}^{\infty} \sum_{i=0}^{\infty} \sum_{j=0}^{\infty} \frac{(-1)^{m+i+1}}{m} (1 + \lambda)^j \left(\frac{x - \gamma}{\beta}\right)^{\alpha(i+j+1)-1} \tag{13}$$

3.2. Quantile function and random number generation

The random number of the DILLog distribution was generated by inverting the CDF expressed on Equation 5. For this, let us suppose $F(x) = U$, where U is the function that follows the uniform distribution in $[0, 1]$.

$$F(x) = \frac{1}{\ln(1 + \lambda)} \ln \left(\frac{1 + (1 + \lambda) \left(\frac{x - \gamma}{\beta}\right)^{\alpha}}{1 + \left(\frac{x - \gamma}{\beta}\right)^{\alpha}} \right) = U$$

$$Q(X) = \gamma + \beta \left(\frac{\exp\{U \ln(1 + \lambda) - 1\}}{1 + \lambda - \exp\{U \ln(1 + \lambda)\}} \right)^{\frac{1}{\alpha}} \tag{14}$$

The expression in Equation 14 is serves as the quantile function which used is also used to generates random numbers that follow the DILLog distribution. By specifying the parameter values for this distribution, a set of random numbers describing the future scenario can be generated using simulation.

4. Method of parameter estimation

The maximum likelihood estimates (MLEs) of the parameters involved in the DILLog distribution are given as follows: Let X_1, X_2, \dots, X_n be a random sample of observed values from a DILLog distributed random variable X . Then the likelihood function is given by

$$L = \left(\frac{\alpha \lambda}{\beta \ln(1 + \lambda)} \right)^n \prod_{i=1}^n \left[\frac{\left(\frac{x_i - \gamma}{\beta}\right)^{\alpha - 1}}{\left(1 + \left(\frac{x_i - \gamma}{\beta}\right)^{\alpha}\right) \left(1 + (1 + \lambda) \left(\frac{x_i - \gamma}{\beta}\right)^{\alpha}\right)} \right] \tag{15}$$

After taking the natural logarithm of Equation 15 on both sides, the log-likelihood function of the DILLog distribution becomes

$$\ln L = n \ln \left(\frac{\alpha \lambda}{\beta \ln(1 + \lambda)} \right) + (\alpha - 1) \sum_{i=1}^n \ln \left(\frac{x_i - \gamma}{\beta} \right) - \sum_{i=1}^n \ln \left(1 + \left(\frac{x_i - \gamma}{\beta}\right)^{\alpha} \right) - \sum_{i=1}^n \ln \left(1 + (1 + \lambda) \left(\frac{x_i - \gamma}{\beta}\right)^{\alpha} \right) \tag{16}$$

The components of the score vectors to estimate the parameter of the distribution are given by the partial derivative with respect to the parameters as:

$$\frac{\partial \ln L}{\partial \alpha} = \frac{n}{\alpha} + \sum_{i=1}^n \ln \left(\frac{x_i - \gamma}{\beta} \right) - \sum_{i=1}^n \left(1 + \left(\frac{x_i - \gamma}{\beta} \right)^\alpha \right)^{-1} \left(\frac{x_i - \gamma}{\beta} \right)^\alpha \ln \left(\frac{x_i - \gamma}{\beta} \right) \quad (17)$$

$$- (1 + \lambda) \sum_{i=1}^n \left(1 + (1 + \lambda) \left(\frac{x_i - \gamma}{\beta} \right)^\alpha \right)^{-1} \left(\frac{x_i - \gamma}{\beta} \right)^\alpha \ln \left(\frac{x_i - \gamma}{\beta} \right)$$

$$\frac{\partial \ln L}{\partial \beta} = -\frac{n}{\beta} - \left(\frac{n(\alpha - 1)}{\beta} \right) + \frac{\alpha}{\beta} \sum_{i=1}^n \left(1 + \left(\frac{x_i - \gamma}{\beta} \right)^\alpha \right)^{-1} \left(\frac{x_i - \gamma}{\beta} \right)^\alpha \quad (18)$$

$$+ \frac{\alpha(1 + \lambda)}{\beta} \sum_{i=1}^n \left(1 + (1 + \lambda) \left(\frac{x_i - \gamma}{\beta} \right)^\alpha \right)^{-1} \left(\frac{x_i - \gamma}{\beta} \right)^\alpha$$

$$\frac{\partial \ln L}{\partial \gamma} = -\frac{\alpha - 1}{\beta} \sum_{i=1}^n \left(\frac{x_i - \gamma}{\beta} \right)^{-1} + \frac{\alpha}{\beta} \sum_{i=1}^n \left(1 + \left(\frac{x_i - \gamma}{\beta} \right)^\alpha \right)^{-1} \left(\frac{x_i - \gamma}{\beta} \right)^{\alpha - 1} \quad (19)$$

$$+ \frac{\alpha(1 + \lambda)}{\beta} \sum_{i=1}^n \left(1 + (1 + \lambda) \left(\frac{x_i - \gamma}{\beta} \right)^\alpha \right)^{-1} \sum_{i=1}^n \left(\frac{x_i - \gamma}{\beta} \right)^{\alpha - 1}$$

$$\frac{\partial \ln L}{\partial \lambda} = -\frac{n}{(1 + \lambda)(\ln(1 + \lambda))} + \sum_{i=1}^n \left(1 + (1 + \lambda) \left(\frac{x_i - \gamma}{\beta} \right)^\alpha \right)^{-1} \left(\frac{x_i - \gamma}{\beta} \right)^\alpha \quad (20)$$

The parameters of the DILLog distribution are estimated by solving the nonlinear system of equations equating the score vector to zero. As these equations do not yield closed-form solutions, various numerical optimization techniques can be applied. Standard methods include the Newton-Raphson iterative method, which uses first and second derivatives for rapid convergence; the Fisher Scoring method, a variant of Newton-Raphson, which uses the expected information matrix to improve stability; the Broyden-Fletcher-Goldfarb-Shanno (BFGS) algorithm, a quasi-Newton approach, which approximates the Hessian without requiring second derivatives; and the Nelder-Mead simplex method, a derivative-free technique suitable for non-differentiable or noisy likelihood surfaces. Depending on the problem context and computational considerations, any of these methods may be used to obtain the maximum-likelihood estimate of the distribution parameters.

5. Simulation study

To test the performance of the maximum likelihood estimate method presented in the previous section, a simulation study is performed. For this, the suggested quantile function of the new distribution was used to generate random numbers that follow the DIL-

Log distribution. Three distinct parameter sets were selected to create random samples, each representing different shapes and scales of the DILLog distribution. The first set ($\gamma = 1.0, \alpha = 2.0, \beta = 0.5, \lambda = 1.0$) corresponds to a distribution with a relatively higher shape parameter, indicating a more peaked and less skewed behavior. The second set ($\gamma = 2.0, \alpha = 1.0, \beta = 0.6, \lambda = 2.0$) models a distribution shifted to the right with moderate scale and moderate inflation effects. The third set ($\gamma = 1.0, \alpha = 1.0, \beta = 0.7, \lambda = 3.0$) features a lower shape parameter with a larger scale and higher inflation parameter, resulting in a heavier tail and greater skewness. For each parameter configuration, random samples of sizes $n = 50, 100,$ and 500 were generated to assess the robustness of the estimation procedure across varying distributional shapes and data volumes. Each sample size was repeated $N = 1000$ times. The MLE technique was used to estimate the parameters, the algorithm used was Limited-memory BFGS with Box (L-BFGS-B) constraints. The mean estimated values of the parameters were tested using bias of estimation, variance of difference, and mean squared errors (MSEs). Tables 1 to 3 present the numerical summary of the simulation study results for Set I, Set II, and Set III separately.

Table 1. Simulation results for set I

| Sample Size | Parameter | True Value | Estimate | Bias | Variance | MSE |
|-------------|-----------|------------|----------|---------|--------------------|----------------------|
| 50 | γ | 1.0 | 1.0315 | 0.0315 | 0.0011 | 0.0020 |
| | α | 2.0 | 3.7656 | 1.7656 | 1.6062 | 4.7234 |
| | β | 0.5 | 0.5798 | 0.0798 | 0.0037 | 0.0101 |
| | λ | 1.0 | 0.4276 | -0.5724 | 0.3182 | 0.6458 |
| 100 | γ | 1.0 | 1.0143 | 0.0143 | 0.0002 | 0.0004 |
| | α | 2.0 | 3.9868 | 1.9868 | 2.3014 | 6.2489 |
| | β | 0.5 | 0.6297 | 0.1297 | 0.0028 | 0.0196 |
| | λ | 1.0 | 0.6037 | -0.3963 | 0.4832 | 0.6403 |
| 500 | γ | 1.0 | 1.0029 | 0.0029 | 6×10^{-6} | 1.4×10^{-5} |
| | α | 2.0 | 3.4113 | 1.4113 | 1.0747 | 3.0665 |
| | β | 0.5 | 0.6788 | 0.1788 | 0.0008 | 0.0328 |
| | λ | 1.0 | 0.3339 | -0.6661 | 0.3276 | 0.7714 |

Among the four parameters, the γ estimates exhibit excellent accuracy, with bias and variance decreasing as the sample size increases, confirming the reliability of its estimation. The α estimates improve significantly with larger sample sizes, as bias reduces and variance remains within a moderate range. Similarly, β estimates show steady improvement, as bias diminishes and variance decreases with increasing sample sizes. Although λ estimates are lower than the actual values, their precision improves as the sample size increases, indicating that larger samples yield more stable estimates.

Table 2. Simulation results for set II

| Sample Size | Parameter | True Value | Estimate | Bias | Variance | MSE |
|-------------|-----------|------------|----------|---------|----------------------|-----------------------|
| 50 | γ | 2.0 | 2.0074 | 0.0074 | 0.0001 | 0.0001 |
| | α | 1.0 | 1.1742 | 0.1742 | 0.3836 | 0.4140 |
| | β | 0.6 | 0.6491 | 0.0491 | 0.0061 | 0.0085 |
| | λ | 2.0 | 1.6870 | -0.3130 | 1.7552 | 1.8531 |
| 100 | γ | 2.0 | 2.0030 | 0.0030 | 9.7×10^{-6} | 1.86×10^{-5} |
| | α | 1.0 | 1.0169 | 0.0169 | 0.3391 | 0.3393 |
| | β | 0.6 | 0.7069 | 0.1069 | 0.0029 | 0.0144 |
| | λ | 2.0 | 1.5438 | -0.4562 | 2.6246 | 2.8327 |
| 500 | γ | 2.0 | 2.0007 | 0.0007 | 5×10^{-6} | 1×10^{-6} |
| | α | 1.0 | 0.8348 | -0.1652 | 0.1523 | 0.1796 |
| | β | 0.6 | 0.7711 | 0.1711 | 0.0009 | 0.0302 |
| | λ | 2.0 | 1.1891 | -0.8109 | 2.9235 | 3.5811 |

Table 3. Simulation results for set III

| Sample Size | Parameter | True Value | Estimate | Bias | Variance | MSE |
|-------------|-----------|------------|----------|---------|----------------------|-----------------------|
| 50 | γ | 1.0 | 1.0062 | 0.0062 | 4.8×10^{-5} | 8.6×10^{-5} |
| | α | 1.0 | 0.9636 | -0.0364 | 0.3245 | 0.3259 |
| | β | 0.7 | 0.7045 | 0.0045 | 0.0097 | 0.0097 |
| | λ | 3.0 | 2.5322 | -0.4678 | 2.7415 | 2.9603 |
| 100 | γ | 1.0 | 1.0028 | 0.0028 | 7×10^{-6} | 1.47×10^{-5} |
| | α | 1.0 | 0.8467 | -0.1533 | 0.1475 | 0.1710 |
| | β | 0.7 | 0.7760 | 0.0760 | 0.0034 | 0.0091 |
| | λ | 3.0 | 2.4397 | -0.5603 | 3.8750 | 4.1889 |
| 500 | γ | 1.0 | 1.0006 | 0.0006 | 2.5×10^{-7} | 5.7×10^{-7} |
| | α | 1.0 | 0.7389 | -0.2611 | 0.0819 | 0.1500 |
| | β | 0.7 | 0.8330 | 0.1330 | 0.0013 | 0.0189 |
| | λ | 3.0 | 2.1278 | -0.8722 | 3.2656 | 4.0263 |

6. Application to survival and demographic data

To test the flexibility of the DILLog distribution, two real data sets have been applied. The parameters of the proposed model and the comparative models were obtained by maximizing the negative log-likelihood as the Objective function using the OPTIM function in the Adequacy Model (Marinho et al., 2019) of the R package for probability distributions (R Core Team, 2025). The AIC, BIC, KS, and AD tests were applied as validity tools to show the flexibility and suitability of the proposed model. The KS test value measures the maximum difference between the empirical and model CDFs. The AD statistics are a weighted measure of the difference between the empirical and model CDFS.

The first data set is the age at menarche of Nepalese females, taken from the Nepal Demographic and Health Survey 2022 (MoHP, 2023). It contains 14,349 data points on the age at menarche of Nepalese females. The second data set is from Susarla and Vanryzin (1978) and comprises 46 data points on the survival times (months) of patients with melanoma disease. This second data set was recently used by Mohammad and Gaire (2025). Table 4 presents the summary statistics for both data sets.

Table 4. Summary statistics of survival time for melanoma disease and age at menarche

| Statistics | Min | Q1 | Median | Mode | Mean | Q3 | Sk | K | max |
|------------|------|------|--------|------|-------|-------|-------|-------|------|
| Melanoma | 3.25 | 6.75 | 12.88 | 4.75 | 15.66 | 22.31 | 1.412 | 2.220 | 58.5 |
| Menarche | 7 | 13 | 14 | 14 | 13.96 | 15 | 0.623 | 1.238 | 25 |

Both data sets were presented using the box-and-whisker plot in Figure 6. The first plot illustrates the age at menarche for Nepalese girls and shows skewness as well as outliers on both sides. Similarly, the second plots presents a box-and-whisker plot of melanoma survival time, which is also right-skewed and contains one outlier.

The result obtained by fitting the proposed model was compared with a three-parameter LLog distribution with PDF in Equation 3, a four-parameter Transmuted Log-Logistic (TrL-Log) distribution with PDF expressed in Equation 23 taken from Aryal (2013), and a five-parameter Kumarswamy Log-Logistic (KuLLog) distribution expressed in Equation 24, taken from De-Santana et al. (2012).

$$f(x)_{TrLLog} = \frac{\alpha (1 + \lambda) \left(\frac{x-\gamma}{\beta}\right)^{\alpha-1} + (1 - \lambda) \left(\frac{x-\gamma}{\beta}\right)^{2\alpha-1}}{\beta \left[1 + \left(\frac{x-\gamma}{\beta}\right)^\alpha\right]^3} \tag{23}$$

$$f(x)_{KuLLog} = \frac{ab\alpha}{\beta} \left(\frac{x-\gamma}{\beta}\right)^{a\alpha-1} \left[1 + \left(\frac{x-\gamma}{\beta}\right)^\alpha\right]^{-(a+1)} \left\{1 - \left(\frac{\left(\frac{x-\gamma}{\beta}\right)^\alpha}{1 + \left(\frac{x-\gamma}{\beta}\right)^\alpha}\right)^a\right\}^{b-1} \tag{24}$$

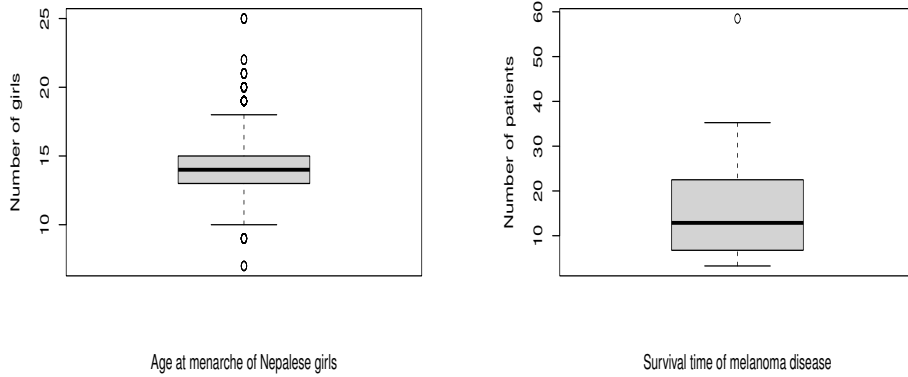


Figure 6. Box-and-whisker plots

Both TrLLog and KuLLog distributions were recently used to modeled demographic data such as the age at menopause (Gaire et al., 2023), the age of a mother at birth of a child (Gaire et al, 2024b), and the age at menarche (Gaire et al., 2024c).

Table 5 presents the goodness-of-fit test statistics and parameter estimates for the DILLog model, along with those of competing models. For the survival time data of melanoma patients, the DILLog distribution shows superior performance, with the lowest AIC (332.2680) and BIC (339.5830), as well as the smallest KS statistic (0.0586) and AD statistic (0.1798) among the models compared. Although the associated p-values for the KS and AD tests are relatively high (e.g. 0.9975 for KS and 0.9950 for AD), it is essential to emphasize that these p-values do not directly measure model fit. Instead, they indicate insufficient evidence to reject the null hypothesis that the data follow the DILLog distribution. A high p-value, in this context, reflects the absence of strong evidence against the model but does not confirm its adequacy. The model selection should primarily be based on comparative fit measures such as AIC, BIC, and the observed values of KS and AD statistics, rather than the magnitude of the p-values. Based on these criteria, the DILLog model emerges as the most appropriate choice for these data sets.

Similarly, Table 6 presents goodness-of-fit test statistics and parameter estimates for the DILLog model and other comparative models of the age at menarche of Nepalese girls. For this data set, multiple validity criteria confirm that the proposed DILLog distribution performs best in testing age-at-menarche data. The proposed model exhibits the minimum AIC (112102) and BIC (112135) values. For the age-at-menarche data of Nepalese girls, the DILLog model has the lowest KS value (0.1359) among the compared models, indicating the best fit. For this data set, the DILLog shows the lowest AD statistic (587.8871) among all compared models, showing it provides the best fit to the data. The comparative analysis reveals that the DILLog distribution provides the best overall fit among the models consid-

Table 5. Estimated parameter values and various goodness-of-fit test statistics for survival time for melanoma disease

| Parameters / Test Statistics | LLog | KuLLog | TrLLog | DILLog |
|------------------------------|---------------|----------------|----------------|----------------|
| α | 1.727 | 0.175 | 1.727 | 5.894 |
| β | 8.934 | 8005.975 | 8.986 | 36.694 |
| γ | 2.683 | 3.164 | 2.683 | 0.661 |
| λ | – | – | 0.01 | 859554.2 |
| a | – | 8.026 | – | – |
| b | – | 81477.4 | – | – |
| AIC | 335.1957 | 334.2525 | 337.1959 | 332.268 |
| BIC | 340.6817 | 343.3957 | 344.5104 | 339.583 |
| KS | 0.078 (0.941) | 0.0633 (0.993) | 0.0782 (0.941) | 0.0586 (0.997) |
| AD | 0.397 (0.851) | 0.259 (0.965) | 0.397 (0.851) | 0.1798 (0.995) |

Table 6. Estimated parameter values and various test statistics for the age at menarche

| Parameters / Test Statistics | LLog | KuLLog | TrLLog | DILLog |
|------------------------------|-----------------|-----------------|-----------------|-----------------|
| α | 9.829 | 7.742 | 13.576 | 13.535 |
| β | 8.408 | 12.197 | 12.929 | 10.594 |
| γ | 5.418 | 0.010 | 0.010 | 5.012 |
| λ | – | – | –0.971 | 141.899 |
| a | – | 4.502 | – | – |
| b | – | 2.603 | – | – |
| AIC | 112511.9 | 112154.1 | 112397.4 | 112102.0 |
| BIC | 112536.9 | 112195.7 | 112430.7 | 112135.0 |
| KS | 0.143 (0.000) | 0.140 (0.000) | 0.152 (0.000) | 0.136 (0.000) |
| AD | 618.519 (0.000) | 596.077 (0.000) | 626.275 (0.000) | 587.887 (0.000) |

ered, as indicated by its lowest AIC, BIC, KS, and AD values. These results highlight the flexibility and robustness of the DILLog model in capturing the underlying structure of the menarche data. Although the KS test yields very small p-values of 0.0000, this should not be viewed as a sign of a poor model fit. Rather, such p-values are commonly observed in large samples, where even minor deviations from the theoretical distribution become statistically significant. Notably, model selection in this context relies primarily on AIC, BIC, KS, and AD values, rather than the associated p-values. Therefore, despite the limitations of p-values in large sample settings, the DILLog model remains the most suitable and preferred choice for the menarche data.

Figure 7 presents the histogram of observed number of melanoma survivors together with the fitted curves from different models. The DILLog model is found to better fit the data across multiple validity criteria, as confirmed by the fitted graphs and the test results.

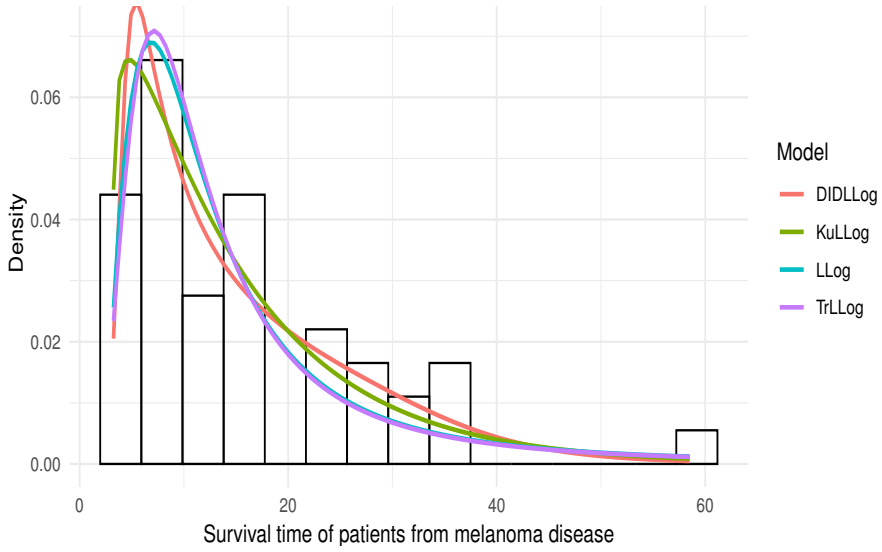


Figure 7. Histogram of observed number of patients with survival times for melanoma disease along with fitted PDFs of competing distributions

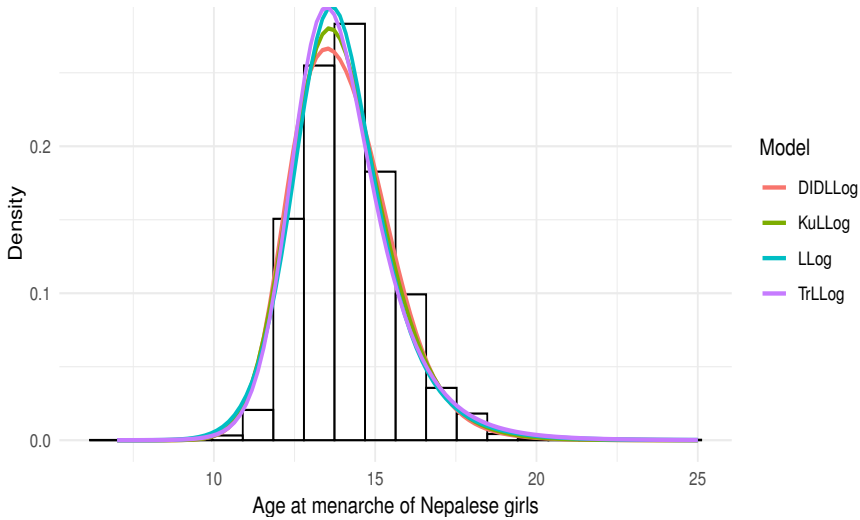


Figure 8. Histogram of observed number of girls with age-at-menarche along with fitted PDFs of competing distributions

Similarly, the histogram of the observed number of Nepalese girls at age at menarche together with the fitted curves from different models was presented on Figure 8. The DILLog model is found to better fit the data across multiple validity criteria, as confirmed by the fitted graphs and the test results.

7. Conclusions

This study introduced a new probability distribution, the DILLog distribution, formulated as a sub-model within the DI family of distributions, with the LLog distribution serving as its baseline due to its recognized flexibility and practical relevance. Several fundamental statistical properties of the proposed model were derived, providing a comprehensive theoretical foundation. Parameter estimation was carried out using the maximum likelihood method, ensuring efficient and reliable estimation across competing models. To evaluate the robustness and practical applicability of the DILLog distribution, both numerical simulations and empirical analyses based on two real data sets were conducted. The results from multiple goodness-of-fit tests consistently demonstrated that the proposed DILLog model outperformed the selected models, confirming its superior flexibility and fitting capability. The findings indicate that the DILLog distribution is a valuable addition to the DI family and holds strong potential for broader applications in statistical modeling and data analysis.

Funding

This research was supported by the Mini Research Grant provided by the Research and Development Unit of Khwopa Engineering College, Bhaktapur, Nepal (Grant Number: KhEC-SSR-08182-009).

Acknowledgment

The author expresses sincere gratitude to Khwopa Engineering College for providing valuable academic resources and a supportive research environment.

References

- Adeyinka, F. S., Olapade, A. K., (2019). On transmuted four parameters generalized Log-Logistic distribution. *International Journal of Statistical Distributions and Applications*, 5(2), pp. 32–37.
- Alodat, M. D. T., Al-Rawwash, M., (2021). A proposed mechanism for skewing symmetric distributions. *Communications in Statistics-Theory and Methods*, 50(11), pp. 2674–2695.
- Aryal, G. R. (2013). Transmuted log-logistic distribution. *Journal of Statistics Applications and Probability*, 2(1), pp. 11–20.
- De-Santana, T. V. F., Ortega, E. M., Cordeiro, G. M. and Silva, G. O., (2012). The Kumaraswamy-log-logistic distribution. *Journal of Statistical Theory and Applications*, 11(3), pp. 265–291.
- Eugene, N., Lee, C. and Famoye, F., (2002). Beta-normal distribution and its applications. *Communications in Statistics-Theory and Methods*, 31(4), pp. 497–512.

- Gaire, A. K., (2023). Skew Lomax distribution, parameter estimation, its properties, and applications. *Journal of Science and Engineering*, 10, pp. 1–11.
- Gaire, A. K., Aryal, R., (2015). Inverse Gaussian model to describe the distribution of age-specific fertility rates of Nepal. *Journal of Institute of Science and Technology*, 20(2), pp. 80–83.
- Gaire, A. K., Gurung, Y. B., (2024a). Rayleigh generated Log-Logistic distribution: Properties and performance analysis. *Istatistik Journal of Turkish Statistical Association*, 15(1), pp. 13–28.
- Gaire, A. K., Gurung, Y. B., (2024b). Skew Log-logistic distribution: Properties and application. *Statistics in Transition New Series*, 25(1), pp. 43–62.
- Gaire, A. K., Gurung, Y. B., and Bhusal, T. P., (2024a). Age at first marriage of Nepalese women: a statistical analysis (status, differential, determinants, and distributional pattern). *Journal of Population and Social Studies*, 32, pp. 308—328.
- Gaire, A. K., Gurung, Y. B., and Bhusal, T. P., (2023). Stochastic modeling of age at menopause for Nepalese women and development of menopausal life table. *Global Health Economics and Sustainability*. 1(2), pp. 1–11.
- Gaire, A. K., Gurung, Y. B., and Bhusal, T. P., (2024b). Fertility model evolution: a survey on mathematical models of age-specific fertility with application to Nepalese and Malaysian data. *Global Health Economics and Sustainability*. 3(1), pp. 222–234.
- Gaire, A. K., Gurung, Y. B., Bhusal, T. P., (2024c). Stochastic modeling of age at menarche for Nepalese girls and developing menarchial life table. *Population Review*, 63(2), pp. 146-161.
- Gaire, A. K., Thapa G. B. and KC, S., (2019). *Preliminary results of Skew Log-logistic distribution, properties, and application. Proceeding of the 2nd International Conference on Earthquake Engineering and Post Disaster Reconstruction Planning, 25–27 April 2019, Bhaktapur, Nepal*, pp. 37–43.
- Gaire, A. K., Thapa, G. B. and KC, S., (2022). Mathematical modeling of age-specific fertility rates of Nepali mothers. *Pakistan Journal of Statistics and Operation Research*, 18(2), pp. 417–426. <https://doi.org/10.18187/pjsor.v18i2.3319>.
- Gui, W., (2013). Marshall-Olkin extended log-logistic distribution and its application in minification processes. *Applied Mathematical Science*, 7(80), pp. 3947–3961.
- Hemeda, S., (2018). Additive Weibull Log Logistic distribution: Properties and application. *Journal of Advanced Research in Applied Mathematics and Statistics*, 3(4), pp. 8–15.
- Hamedani, G., (2013). The Zografos-Balakrishnan log-logistic distribution: Properties and applications. *Journal of Statistical Theory and Applications*, 12(3), pp. 225–244.
- Jones, M., (2004). Families of distributions arising from distributions of order statistics. *Test*, 13(1), pp. 1–43.

- Lemonte, A. J., (2014). The Beta log-logistic distribution. *Brazilian Journal of Probability and Statistics*, 28(3), pp. 313–332.
- Marinho, P. R. D., Silva, R. B., Bourguignon, M., Cordeiro, G. M., and Nadarajah, S., (2019). AdequacyModel: An R package for probability distributions and general-purpose optimization. *PLoS One*, 14(8), e0221487.
- Marshall, A. W., Olkin, I., (1997). A new method for adding a parameter to a family of distributions with application to the exponential and Weibull families. *Biometrika*, 84(3), pp. 641–652.
- Ministry of Health and Population, New ERA, and ICF International Inc. (2023). Nepal demographic and health survey 2022. *Kathmandu, Nepal: Ministry of Health and Population*.
- Mohammad, S., Cooray, K., (2025). Modeling actuarial data using iterated trigonometric distributions. *Communications in Statistics-Theory and Methods*, 54(16), pp. 5112–5128.
- Mohammad, S., Gaire, A.K. (2025). Exponential Arctan-G Family of Distribution with Properties and Applications, *Journal of Probability and Statistics*, 25(1), pp.–13.
- R Core Team, (2025). *R: A language and environment for statistical computing*. R Foundation for Statistical Computing, Vienna, Austria.
- Susarla, V., Van Ryzin, J., (1978). Empirical Bayes estimation survival distribution function from right censored data. *Anal. Statist*, 6, pp. 740–755.
- Tahir, M. H., Mansoor, M., Zubair, M. and Hamedani, G., (2014). McDonald log-logistic distribution with an application to breast cancer data. *Journal of Statistical Theory and Applications*, 13(1), pp. 65–82.
- Zografos, K., Balakrishnan, N., (2009). On families of Beta-and generalized Gamma-generated distributions and associated inference. *Statistical Methodology*, 6(4), pp. 344–362.